Chapter 2

A Convergent Collocation Approach for Generalized Fractional Integro-Differential Equations Using Jacobi Poly-Fractonomials

2.1 Introduction

Here, we consider the GFIDEs in terms of the B-operator [30]. The B-operator reduces to Caputo derivative and Riemann Liouville derivative for a particular choice of kernel in B-operator. The GFIDEs are solved using the collocation method with Jacobi poly-fractonomials. The GFIDEs converted into a system of algebraic equations and solved them to get the solution of GFIDEs. The main aim of this study is

to describe a possible way to find the approximate solution of defined GFIDEs which is close to the exact solution. Section 1 provides the basic definitions of the operator as given in [30]. Further some basic property about Jacobi poly-fractonomials [112] of the first kind is defined as,

$$P_n^a(x) = (2/T)^a(x)^a J_n^{(-a,a)}(2x/T), \quad x \in [0,T], \tag{2.1}$$

where $J_n^{(-a,a)}(2x/T-1)$ denoted the standard Jacobi polynomial in $[0,T]$ of degree n.

The rest of the chapter is organized as follows: Section 2.2 we have provided Generalized fractional integro-differential equations and some of the basic property of Jacobi poly fractonomials to approximate the function. In Section 2.3 we discussed the procedure to apply Collocation methods for solving GFIDEs. Section 2.4 provides a convergence analysis of the method. In Section 2.5, we have done error analysis in two parts by taking linear and non-linear GFIDEs. Section 2.6 presents five numerical examples that illustrate the accuracy of the proposed method. Finally, in Section 2.7 conclusion is discussed.

2.2 Generalized Fractional Iintegro-Differential Equations

We first define FIDEs in terms of K and A/B-operators. These operators [30] are defined as follows

$$K_P^{\gamma}u(x) = r\int_a^x w_{\gamma}(x,t)u(t)\,dt + s\int_x^b w_{\gamma}(x,t)u(t)\,dt, \quad \gamma > 0, \tag{2.2}$$

where, $x \in [a, b]$, $P =< a, b, r, s >$ denote the all parameters, $w_\gamma(x, t)$ is a kernel defined on the space $I \times I$. We assume that $w_\gamma(x, t)$ and $u(t)$ both are square integrable function such that Eq. (2.2) exists. K operator satisfies the linearity properties, i.e. for any two functions $u_1(t)$ and $u_2(t)$, then

$$K_P^\gamma(u_1(x) + u_2(x)) = K_P^\gamma u_1(x) + K_P^\gamma u_2(x). \tag{2.3}$$

Define, A and B-operators [30] as follows,

$$A_P^\gamma u(x) = D^n K_P^{(n-\gamma)} u(x), \tag{2.4}$$

$$B_P^\gamma u(x) = K_P^{(n-\gamma)} D^n u(x). \tag{2.5}$$

by using Eq. (2.5), Eq. (2.2) can be written as,

$$B_P^\gamma u(x) = r \int_0^x w_{m-\gamma}(x, t) D^n u(t)\, dt + s \int_x^1 w_{m-\gamma}(t, x) D^n u(t)\, dt, \quad \gamma > 0, \tag{2.6}$$

where, $m - 1 < \gamma < m$, m is an integer and $P =< 0, 1, r, s >$ and $D^n u(t)$ denote the n^{th} derivative of the function $u(t)$. In the definition of B-operator, we assume that $D^n u(x)$ is integrable once on domain I. Details about all this operator can be found in [30].

Now, we will define GFIDEs using B-operator as follows

$$(B_P^\gamma u)(x) = (Hu)(x), \quad 0 < \gamma < 1, \tag{2.7}$$

$$u(0) = u_0. \tag{2.8}$$

where

$$(Hu)(x) = \phi(x) + g(x)u(x) + \int_0^x \rho(x,t)G(u(t))dt, \quad 0 < \gamma < 1, \quad x \in I = [0,1], \tag{2.9}$$

$$(B_P^{\gamma}u)(x) = r\int_0^x w_{m-\gamma}(x,t)D^n u(t)dt + s\int_x^1 w_{m-\gamma}(t,x)D^n u(t)dt, \quad \gamma > 0, \tag{2.10}$$

where, function $\phi(x)$ and $g(x)$ are square integrable functions in I with, $g(x) \neq 0$, and $u(x)$ is unknown. This problem is considered in the interval $[0,1]$ and kernel $\rho(x,t)$ is weakly singular of the form

$$\rho(x,t) = (x-t)^{-v}, \quad 0 < v < 1. \tag{2.11}$$

Also, in definition of B-operator, there is another kernel $w_{\gamma}(x,t)$, we have taken kernel $w_{\gamma}(x,t) \in L^2(I \times I)$ and G defined by Eq. (2.10) can be either linear or non-linear operator.

We assume that Eqs. (2.7) and (2.8) have a unique solution for all real value of r and s, either $r = 0$ for all s or $s = 0$ for all r, and one of the special case when $r = 1$ and $s = 0$. The motive is to find the numerical method to solve GFIDEs which is given by Eq. (2.7) and Eq. (2.8).

2.2.1 Preliminaries. Jacobi Poly-Fractonomials and Function Approximation

2.2.1.1 Definition and properties of shifted Jacobi poly-fractonomials

Jacobi poly-fractonomials are the eigenfunctions of the fractional Sturm-Liouville eigen-problems of first kind, which are defined by,

$$P_n^a(x) = (1+x)^a J_n^{-a,a}(x), \quad x \in [-1,1], \quad n = 0,1,2..., \tag{2.12}$$

where $J_n^{-a,a}$ denotes the standard Jacobi polynomial, and n is the degree. $J_n^{-a,a}$ forms Hilbert space in $L^2_{w^2}[-1,1]$, with respect to the weight function $w(t) = (1-t)^{-a}(1+t)^a$, and satisfies orthogonal property with respect to the weight function $w(x)$, i.e.

$$\int_{-1}^{1} J_m^{a,b} J_n^{a,b} w(x)\, dx = Y_n^{a,b} \delta_{nm}, \tag{2.13}$$

where δ_{nm} is the Kronecker delta function, and

$$Y_n^{a,b} = \frac{2^{a+b+1}\Gamma(n+a+1)\Gamma(n+b+1)}{(2n+a+b+1)\Gamma(n+1)\Gamma(n+a+b+1)}, \tag{2.14}$$

is an orthogonally constant.

$$J_n^{a,b}(x) = \frac{\Gamma(n+a+1)}{\Gamma(n+1)\Gamma(n+a+b+1)} \sum_{r=0}^{n} \binom{n}{r} \frac{\Gamma(a+b+n+r+1)\Gamma(n+a+1)}{\Gamma(n+1)\Gamma(r+a+1)} \frac{(x-1)^r}{2^r}, \tag{2.15}$$

is the Jacobi polynomials of degree n and $\binom{n}{r}$ is binomial coefficient defined as, $\binom{n}{r} = \frac{n(n-1)(n-2)...(n-r+1)}{r!}$ and Γ denotes the Euler's gamma function. It has been proved in Ref. [112] that Jacobi poly-fractonomials $P_n^a(x)$ are orthogonal with respect to the weight function, $w(x) = (1-x)^{-a}(1+x)^{-a}$, and form Hilbert space in $L^2_w[-1,1]$. We use the transformation, $x = (2x/T - 1)$ which transforms the standard interval

$[-1,1]$ to $[0,T]$ then we obtain the corresponding shifted Jacobi poly-fractonomials of the first kind

$$\tilde{P}_n^a(x) = \left(\frac{2}{T}\right)^a x^a J_n^{-a,a}\left(\frac{2x}{T}-1\right), \quad x \in [0,T], \quad n = 0,1,2.... \tag{2.16}$$

For the interval $[0,1]$, Eq. (2.16) takes form,

$$\tilde{P}_n^a(x) = (2)^a x^a J_n^{-a,a}(2x-1), \quad x \in [0,1], \quad n = 0,1,2,3...,$$

$\tilde{P}_n^a(x)$ can be written in series combination using the definition of Jacobi polynomial,

$$\tilde{P}_n^a(x) = \frac{2^a\Gamma(n-a+1)}{\Gamma(n+1)}\sum_{r=0}^{n}\binom{n}{r}\frac{\Gamma(n+r+1)}{\Gamma(r-a+1)}x^a(x-1)^r. \tag{2.17}$$

Corresponding to weight function $\tilde{w}(x) = (1-x)^{-a}x^{-a}$ we get the orthogonal property

$$\int_{-1}^{1}\tilde{P}_n^a(x)\tilde{P}_m^a(x)w(x)dx = Y_n^{-a,a}\delta_{nm}, \tag{2.18}$$

$$\int_{-1}^{1}\tilde{P}_n^a(x)\tilde{P}_m^a(x)w(x)dx = 2^{-2a+1}\int_{0}^{1}\tilde{P}_n^a(x)\tilde{P}_m^a(x)\tilde{w}(x)dx, \tag{2.19}$$

Let $X = L^2(I)$ be the square integrable over interval I, and for $u_1, u_2 \in X$, the inner product is defined by

$$< u_1, u_2 >= \int_0^1 u_1(t)u_2(t)dt, \tag{2.20}$$

and corresponding norm is defined as follows,

$$\|u\|_2 = \left(\int_0^1 |u(t)|^2 dt\right)^{\frac{1}{2}}.$$

2.2.2 Function Approximation Using Jacobi Poly-fractonomials

Any function $u(x) \in L^2(I)$ can be written as,

$$u(x) = \sum_{k=0}^{\infty} c_k \tilde{P}_k^a(x), \tag{2.21}$$

In practice, if we consider only the first $(N+1)$ terms of $\tilde{P}_k^a(x)$. Then

$$u(x) \approx u_N(x) = \sum_{k=0}^{N} c_k \tilde{P}_k^a(x), \tag{2.22}$$

where c_k nd $\tilde{P}_k^a(x)$ are given by

$$c_k = [c_1, c_2, c_3, ...c_N]^T, \quad \tilde{P}_k^a(x) = [\tilde{P}_0^a(x), \tilde{P}_1^a(x), ...\tilde{P}_N^a(x)]^T.$$

Theorem 2.2.1. Let $u(x)$ be a real, sufficiently smooth function, and $u_N(x) = C^T \tilde{P}_n^a(x)$ denote the shifted Jacobi poly-fractonomials in the expansion of $u(x)$, where

$C = [c_0, c_1, c_2...c_N]^T$, and $c_r = \frac{2^{-2a+1}}{Y_n^{-a,a}} \int_0^1 u(x)\tilde{w}(x)\tilde{P}_k^a(x)$.

Theorem 2.2.2. Let $u(x) \in L^2[0,1] \cap C[0,1]$ then Jacobi –approximation of $u(x)$ given by Eq. (2.22) converges uniformly and we have

$$\|c_r\| \leq \frac{\zeta 2^{-a}(2n+1)(n!)^2\Gamma(1-a)}{\Gamma(n+a+1)\Gamma(2-a+n)\Gamma(1-a+n)}. \tag{2.23}$$

Proof. A function $u(x) \in L^2[0,1] \cap C[0,1]$ can be written by Eq. (2.22), and the coefficient is determined by

$$c_r = \frac{1}{\|\tilde{P}_r^a(x)\|_2^2} \int_0^1 u(x)\tilde{w}(x)\tilde{P}_r^a(x)dx, \tag{2.24}$$

$$c_r \leq \frac{\sup|u(x)|}{\|\tilde{P}_r^a(x)\|_2^2} \int_0^1 |\tilde{w}(x)\tilde{P}_r^a(x)|dx. \tag{2.25}$$

Since, $\sup|u(x)| \leq \zeta$, so from Eq. (2.25) we get,

$$c_r \leq \frac{\zeta}{\|\tilde{P}_r^a(x)\|_2^2} \int_0^1 |\tilde{w}(x)\tilde{P}_r^a(x)|dx. \tag{2.26}$$

Substituting the value of $w(x)$ and $\tilde{P}_r^a(x)$ Eq. (2.26), we have

$$c_r \leq \frac{\zeta 2^a}{\|\tilde{P}_r^a(x)\|_2^2} \sum_{r=0}^{n} A(r,a,n) \int_0^1 |(1-x)^{-a}x^{-a}(x-1)^r x^a|dx, \tag{2.27}$$

where

$$A(r,a,n) = \sum_{r=0}^{n} \binom{n}{r} \frac{\Gamma(n-a+1)\Gamma(n+r+1)}{\Gamma(n+1)\Gamma(r-a+1)}. \tag{2.28}$$

$$c_r \leq \frac{\zeta 2^a}{\|\tilde{P}_r^a(x)\|_2^2} \sum_{r=0}^{n} A(r,a,n) \frac{(-1)^r}{(1-a+r)}. \tag{2.29}$$

Now, substituting the value of $\|\tilde{P}_r^a(x)\|_2^2$ from Eq. (2.17) and $A(r,a,n)$ from Eq. (2.27) in Eq. (2.29), we have

$$c_r \leq \frac{\zeta 2^a 2^{-2a+1}}{Y_n^{-a,a}} \sum_{r=0}^{n} \binom{n}{r} A(r,a,n) \frac{\Gamma(n-a+1)\Gamma(n+r+1)}{\Gamma(n+1)\Gamma(r-a+1)} \frac{(-1)^r}{(1-a+r)}, \tag{2.30}$$

$$\leq \zeta 2^a 2^{-2a+1} \frac{\Gamma(n-a+1)\Gamma(1-a)\Gamma(n+1)(2n+1)\Gamma(n+1)\Gamma(n+1)}{\Gamma(n+1)\Gamma(1-a+n)\Gamma(2-a+n)2\Gamma(n-a+1)\Gamma(1+a+n)}, \tag{2.31}$$

$$\|c_r\| \leq \zeta 2^{-a} \frac{\Gamma(1-a)(2n+1)(n!)^2}{\Gamma(1-a+n)\Gamma(2-a+n)\Gamma(1+a+n)}. \tag{2.32}$$

From this calculation, we obtain that the partial sum of the coefficient are bounded so $\sum_{r=0}^{n} c_r$ converges absolutely and hence, $\sum_{r=0}^{n} c_r \tilde{P}_r^a(x)$ converges uniformly to $u(x)$.

2.3 Collocation Method for GFIDEs

In this part, we describe the collocation method for solving GFIDEs given by Eq. (2.7) and Eq. (2.8). Collocation methods is based on projection method in which we take a finite dimensional basis to express the approximate solution, and is believed to be close to the true solution. With the help of this family of function, we approximate the solution of the GFIDEs given by Eq. (2.7) and Eq. (2.8). Using Eq. (2.22), we now approximate $u(x)$ as,

$$u_N(x) = \sum_{r=0}^{N} c_r \tilde{P}_r^a(x), \tag{2.33}$$

where c_r are unknown expansion coefficients, which are to be determined. It should be noted that the approximate solution $u_N(x)$ satisfies the homogeneous initial condition. Replacing the exact solution $u(x)$ by approximate solution $u_N(x)$ in Eq.

(2.7), we get

$$(B_P^{\gamma} u_N)(x) = (H u_N)(x), \quad 0 < \gamma < 1, \tag{2.34}$$

and

$$u_N(0) = u_0. \tag{2.35}$$

If we are given non-homogeneous initial conditions, $u_N(0) = u_0 \neq 0$, then first we will make it homogeneous by the transformation $\tilde{u}_N(x) \approx u(x) - u_0$ and then replace $u(x)$ by $\tilde{u}_N(x)$. This transformation was considered as Jacobi Poly-fractonomials basis is defined on homogenous initial conditions. From Eqs. (2.34) and (2.35), we have

$$(B_P^{\gamma} \sum_{r=0}^{N} c_r \tilde{P}_r^a(x)) = (H(\sum_{r=0}^{N} c_r \tilde{P}_r^a(x)))(x), \quad 0 < \gamma < 1, \tag{2.36}$$

and

$$\sum_{r=0}^{N} c_r \tilde{P}_r^a(x_0) = u_0. \tag{2.37}$$

To apply collocation method, the node points $x_t \in I = [0, 1]$, are chosen such that

$$(B_P^{\gamma} \sum_{r=0}^{N} c_r \tilde{P}_r^a(x_t)) = (H(\sum_{r=0}^{N} c_r \tilde{P}_r^a(x)))(x_t), \quad t = 0, 1, 2...N-1, \tag{2.38}$$

and

$$\sum_{r=0}^{N} c_r \tilde{P}_r^a(0) = u_0. \tag{2.39}$$

Eq. (2.38) and Eq. (2.39) form a system of linear equation in unknown coefficients c_r and we solve this system of linear equation using any standard method to find the coefficient c_r. And hence, the approximate solution is obtained.

2.4 Convergence Analysis

In this part, we have calculated the convergence analysis of the proposed method. For this, we approximate the function by its derivative and tried to show that its infinite sum is bounded. To study the convergence analysis of the presented method for solving GFIDEs, we will use the following Lemmas

Lemma 2.4.1. Let, $X = L^2(I)$, denote the vector space of square-integrable functions on $I = [0, 1]$ and ζ be a Volterra integral operator on X defined by

$$\zeta u(x) = \int_0^x \rho(x,t)u(t)dt, \forall u \in X, \tag{2.40}$$

with kernel $\rho(x,t)$ satisfying $\int_0^1 \int_0^1 |\rho(x,t)|^2 dx\ dt = L_1^2$ or $\sup_{x,t} \rho(x,t) = L_1$, where L_1 is a constant. Then $\zeta : L^2(I) \to L^2(I)$ is bounded, That is,

$$\|\zeta u\|_2 \leq L_1 \|u\|_2.$$

Lemma 2.4.2. Let $u(x)$ be sufficiently differentiable function in $L^2(I)$, and $\frac{du_N}{dx}$ be the approximation of $\frac{du}{dx}$. Assume that $\frac{du}{dx}$ is bounded by a constant C, i.e. $|\frac{du}{dx}| \leq C$, then we have

$$\left| \frac{du}{dx} - \frac{du_N}{dx} \right|_2^2 \leq C^2 \frac{\Gamma(1-a)(1+2N)(N!)^2(1+\frac{a}{N})}{\Gamma(1-a+N)\Gamma(2-a+N)\Gamma(1+a+N)}. \tag{2.41}$$

Proof Let,

$$\frac{du}{dx} = \sum_{r=0}^{\infty} c_r \tilde{P}_r^a(x), \tag{2.42}$$

Taking the sum of the above series up to $N-1$ level, and replacing the exact solution by approximate solution, we get

$$\frac{du_N}{dx} = \sum_{r=0}^{N-1} c_r \tilde{P}_r^a(x), \tag{2.43}$$

subtracting Eq. (2.42) from the Eq. (2.43), we get

$$\frac{du}{dx} - \frac{du_N}{dx} = \sum_{r=N}^{\infty} c_r \tilde{P}_r^a(x), \tag{2.44}$$

$$\begin{aligned} \|\frac{du}{dx} - \frac{du_N}{dx}\|_2^2 &= \int_0^1 \left(\frac{du}{dx} - \frac{du_N}{dx}\right)^2 dx \\ &= \int_0^1 \left(\sum_{r=N}^{\infty} c_r \tilde{P}_r^a(x)\right)^2 dx, \end{aligned} \tag{2.45}$$

or

$$\|\frac{du}{dx} - \frac{du_N}{dx}\|_2^2 = \sum_{r=N}^{\infty} \frac{c_r^2}{2^{-2a+1}} Y_r^{-a,a}. \tag{2.46}$$

From Eq.(2.42), we get

$$c_r = \frac{2^{-2a+1}}{Y_r^{-a,a}} \int_0^1 \frac{du}{dx} \tilde{P}_r^a(t) \tilde{w}(t) dt, \tag{2.47}$$

substitute the value of $\tilde{P}_r^a(t)$ from Eq. (2.17) and $\tilde{w}(t) = (1-t)^{-a}(t)^{-a}$ Eq. (2.47), we get

$$\begin{aligned} c_r &= \frac{C2^{-2a+1}}{Y_r^{-a,a}} \int_0^1 \frac{du}{dx} \tilde{P}_r^a(t) \tilde{w}(t) dt, \\ &\leq C2^{-a} \frac{\Gamma(1-a)(2r+1)(\Gamma(r+1))^2}{\Gamma(r+a+1)\Gamma(1-a+r)\Gamma(2-a+r)}, \\ |c_r|^2 &\leq \left(C2^{-a} \frac{\Gamma(1-a)(2r+1)(\Gamma(r+1))^2}{\Gamma(r+a+1)\Gamma(1-a+r)\Gamma(2-a+r)}\right)^2. \end{aligned} \tag{2.48}$$

Thus,

$$\sum_{r=N}^{\infty} \frac{c_r^2}{2^{-2a+1}} Y_r^{-a,a} \leq \Gamma(1-a) \sum_{r=N}^{\infty} C^2 \frac{(2r+1)(r!)^2}{\Gamma(r+a+1)\Gamma(1-a+r)\Gamma(2-a+r)},$$
$$\leq C^2 \frac{\Gamma(1-a)(1+2N)(N!)^2(1+\frac{a}{N})}{\Gamma(N+a+1)\Gamma(1-a+N)\Gamma(2-a+N)}, \quad 0 < a < 1. \tag{2.49}$$

which completes the proof of Lemma (2.4.2).

2.5 Error Analysis

In this part, we have estimated the error analysis by considering the different cases. In linear case, it is done by calculating exact and approximate solution. And in non-linear case, first we prove that it satisfies the Lipschitz condition and then apply the usual process to estimate the error. Let, $E_R(x) = |u(x) - u_R(x)|$ be the error function, where $u(x)$ is exact solution and u_R is the approximate solution. From Eq. (2.7), we get,

$$(B_P^{\gamma} u_N)(x) = H(u_N(x)) = \chi(x) + g(x)u_N(x) + \int_0^x \rho(x,t)\mathcal{G}(u_N(t))dt, \tag{2.50}$$

subtracting Eq. (2.50) from the Eq. (2.7), and after simplifying, we get,

$$g(x)(u(x) - u_N(x)) = \int_0^x \rho(x,t)\mathcal{G}(u(t) - u_N(t))dt - (B_P^{\gamma}(u - u_N))(x). \tag{2.51}$$

After substituting all values,

$$g(x)(E_N(x)) = \int_0^x \rho(x,t)\mathcal{G}(E_N(t))dt - (B_P^{\gamma}(u-u_N))(x), \tag{2.52}$$

$$|g(x)(E_N(x))| \leq |\int_0^x \rho(x,t)\mathcal{G}(E_N(t))dt| + |(B_P^{\gamma}(u-u_N))(x)|. \tag{2.53}$$

Here, we consider two case for the function $\mathcal{G}$.

Case 1. When G satisfies linearity condition, we have,

$$|g(x)E_N(x)| \leq Q|\int_0^x E_N(t)dt| + |(B_P^{\gamma}(u-u_N))(x)|, \tag{2.54}$$

where $Q = \max \rho(x,t)$. Now, by using Gronwall's inequality,

$$\|g(x)E_N(x)\|_2 \leq \|(B_P^{\gamma}(u-u_N))(x)\|_2. \tag{2.55}$$

Now, by using Gronwall's inequality,

$$\|(B_P^{\gamma}(u-u_N))(x)\|_2 \leq \|K_1\|_2 + \|K_2\|_2, \tag{2.56}$$

where K_1 and K_2 are defined by,

$$K_1 = r\int_o^x w_{1-\gamma}(x,t)\mathcal{D}(u(t)-u_N(t))dt, \tag{2.57}$$

and

$$K_2 = s\int_x^1 w_{1-\gamma}(t,x)\mathcal{D}(u(x)-u_N(x))dx. \tag{2.58}$$

Since $w_{(1-\gamma)}(x,t) \in L^2$, then by Lemma (2.4.1) there exist constants k_1, k_2 such that,

$$\|K_1\|_2 \leq k_1\|\mathcal{D}(u(x)-u_N(x))\|_2, \tag{2.59}$$

and

$$\|K_2\|_2 \leq k_2 \|\mathcal{D}(u(x) - u_N(x))\|_2. \tag{2.60}$$

Thus,

$$\|(B_P^{\gamma}(u - u_N))(x)\|_2 \leq \Lambda \|\mathcal{D}(u(x) - u_N(x))\|_2, \quad \Lambda = k_1 + k_2. \tag{2.61}$$

Using Lemma (2.4.2),

$$\|(B_P^{\gamma}(u - u_N))(x)\|_2 \leq \Lambda(C)^2 \frac{\Gamma(1-a)(1+2N)(N!)^2(a+\frac{a}{N})}{\Gamma(1+a+N)\Gamma(1-a+N)\Gamma(2-a+N)}. \tag{2.62}$$

From Eq. (2.55) and (2.61), we have,

$$\|g(x)E_N(x)\|_2 \leq k(C)^2 \frac{\Gamma(1-a)(1+2N)(N!)^2(a+\frac{a}{N})}{\Gamma(1+a+N)\Gamma(1-a+N)\Gamma(2-a+N)}. \tag{2.63}$$

Since $g(x) \neq 0$, therefore $E_N(x) \to 0$ or $u(x) \to u_N(x)$ as $N \to \infty$.

Case 2. When G is nonlinear.

Lipschitz condition: A function $f(x, y)$ satisfies a Lipschitz condition in the variable y on a set D subset of R^2 if there exist a constant $L > 0$ such that,

$$|f(x, y_1) - f(x, y_2)| \leq L|y_1 - y_2|.$$

We assume that G satisfies the Lipschitz condition in variable y so,

$$|G(y_1(t)) - G(y_2(t))| \leq L|y_1(t) - y_2(t)|, \tag{2.64}$$

where L is a Lipschitz constant. From Eq. (2.51), we have

$|g(x)E_N(x)| \leq |\int_0^x \rho(x,t)\mathcal{G}(E_N(t))dt| + |(B_P^{\gamma}(u - u_N))(x)|$,

or,

$|g(x)E_N(x)| \leq LQ|\int_0^x E_N(t)dt| + |(B_P^{\gamma}(u-u_N))(x)|$. Now, following the similar steps

as discussed for Eq. (2.55), the convergence bound can be proved like in Eq. (2.63).

Error estimate In this section, we discuss in general to calculate the error of the given problem. Let $E_N(x) = |u(x) - u_N(x)|$ be denote the error function of $u_N(x)$ to the exact solution $u(x)$. Replacing $u(x)$ by the approximate solution $u_N(x)$ in Eq. (2.7), we obtain

$$(B_P^{\gamma}\gamma_N)(x) + u_N(x) = \chi(x) + g(x)u_N(x) + \int_0^x \rho(x,t)\mathcal{G}(u_N(t))dt, \tag{2.65}$$

with $u(0) = (u)_N$.

Here, $u_N(x)$ is the perturbation function that can be calculated as

$u_N(x) = \chi(x) + g(x)u_N(x) + \int_0^x \rho(x,t)\mathcal{G}(u_N(t))dt - (B_P^{\gamma}u_N)(x)$.

Subtracting Eq. (2.64) from Eq. (2.7), we get

$(B_P^{\gamma}E_N)(x) + u_N(x) = \chi(x) + g(x)E_N(x) + \int_0^x \rho(x,t)\mathcal{G}(E_N(t))dt$,

or

$(B_P^{\gamma}E_N)(x) = \chi(x) + g(x)E_N(x) + \int_0^x \rho(x,t)\mathcal{G}(E_N(t))dt - u_N(x)$, with the initial condition $E_N(0) = (E_0)_N$.

Eq. (2.65) can be solved by apply general methods as we discuss in the Section 4.

2.6 Numerical Examples

To verify the theoretical approximation of the discussed problem, we consider convolution type kernels in GFIDE. The Jacobi poly-fractonomials are considered as a basis to find the approximate solution. We calculate the maximum absolute error by changing the number of elements in the basis in the collocation method. In all numerical results, the number of basis elements and maximum absolute error are denoted by N and MAE respectively.

Example 2.6.1. Consider the problem with $\gamma = 2/3,\ n = 1,$

$$\int_0^x \frac{(a+(1-a)(x-t))^{-\gamma}}{\Gamma(\gamma)}\mathcal{D}^n(u(t))dt + \int_b^x \frac{(a+(1-a)(t-x))^{-\gamma}}{\Gamma(\gamma)}\mathcal{D}^n(u(t))dt$$
$$-u(x) - \int_0^x (x-t)^{-1/2}\mathcal{G}(u(t))dt$$
$$= -x^2 - \frac{16x^{5/2}}{15} + \frac{9x^{4/3}}{2\Gamma(1/3)}$$
$$+ \frac{3(1-x)^{1/3}(1+3x)}{2\Gamma(1/3)}, \tag{2.66}$$

with $u(0) = 0$. This GFIDE has exact solution $u(x) = x^2$ for $a = 0$. In this Example, the exact solution of the problem is given as the second degree polynomial so in the numerical approximation, choice of the basis $N = 2, 3, 4$ are taken and corresponding maximum absolute error are calculated for the different choices of basis and these findings are shown in the Table 2.1. We also observe the variation the approximate solution for the different values of $a = 1/4, 1/8, 1/16, 1/32$ which is shown in Fig. (2.2). The MAE is calculated and the graph of the error is shown in Fig. (2.1). We observe that when a tends to zero error gets reduced and the approximate solution approaches to the exact solution.

TABLE 2.1: MAE of Example 2.6.1 and Example 2.6.2 for different value of N.

N	Example 2.6.1	Example 2.6.2
2	$5.551121e-17$	$5.55112e-17$
3	$2.77556e-17$	$5.55112e-17$
4	$8.32667e-17$	$3.33067e-16$

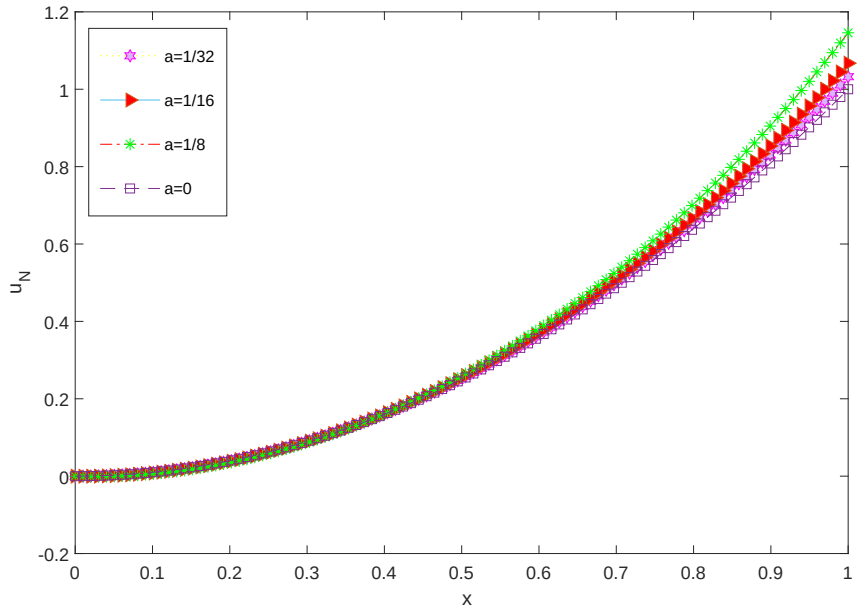

FIGURE 2.1: Plot of approximate solution for different values of a and $N = 2$ for

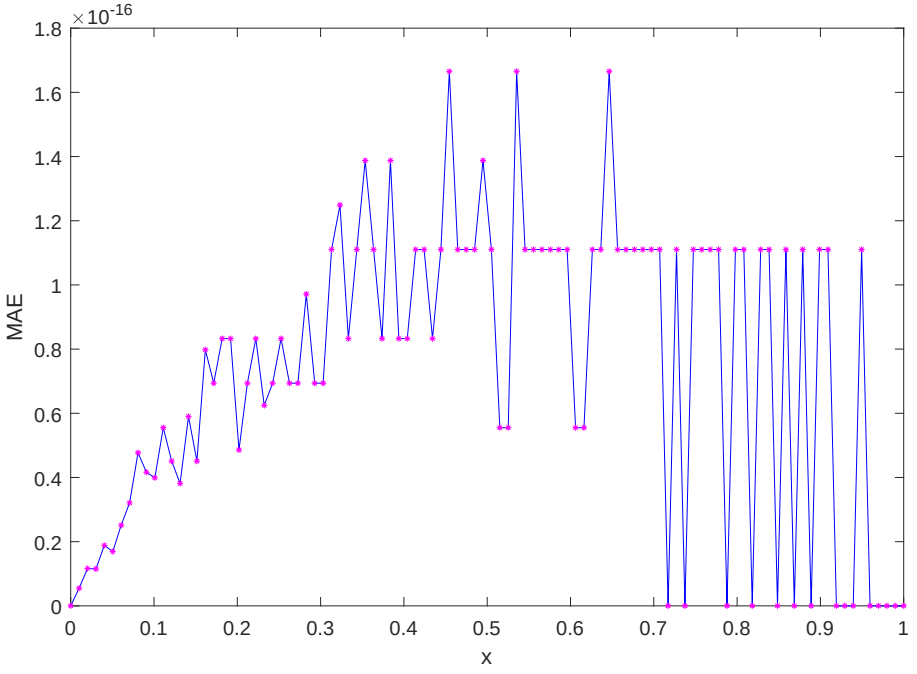

FIGURE 2.2: Plot of MAE of Examples (2.6.1) for $N = 3$, and $\gamma = 2/3$.

Example 2.6.2. Consider the equation with $\gamma = 1/4,\ n = 1$,

$$\begin{aligned}\int_0^x (1-\gamma)(x-t)\mathcal{D}^n(u(t))dt + \int_b^x (1-\gamma)(t-x)\mathcal{D}^n(u(t))dt \\ -u(x) - \int_0^x (x-t)^{-1/3}\mathcal{G}(u(t))dt \\ = -x^2 + \frac{17}{16} - \frac{3x}{2} - \frac{x^3}{2} + \frac{3x^4}{8} \\ - \frac{27}{440}x^{8/3}(11+9x),\end{aligned} \tag{2.67}$$

with initial condition $u(0) = 0$ and the exact solution $x^2 + x^3$. We solve this problem by choosing the different number of basis elements $N = 2, 3, 4$. The corresponding MAE for the different value of N are presented in the Table 2.2 and corresponding graph is shown in Fig. (2.3) for $N = 3$. The approximated solutions of Example (2.6.3) are presented in Fig. (2.4) by taking the different value of $\gamma = 1/4, 1/8, 1/16, 1/32$ and $1/64$. For $\gamma = 1/4$, the numerical solution overlap to the exact solution. Fig. (2.5), shows the relation between the exact and the approximate solutions of the present example. It is clear that whenever γ approaches to $1/4$, the numerical solution converges to the exact solution. The Table 2.3 represents the comparison of the MAE with the method proposed in [1].

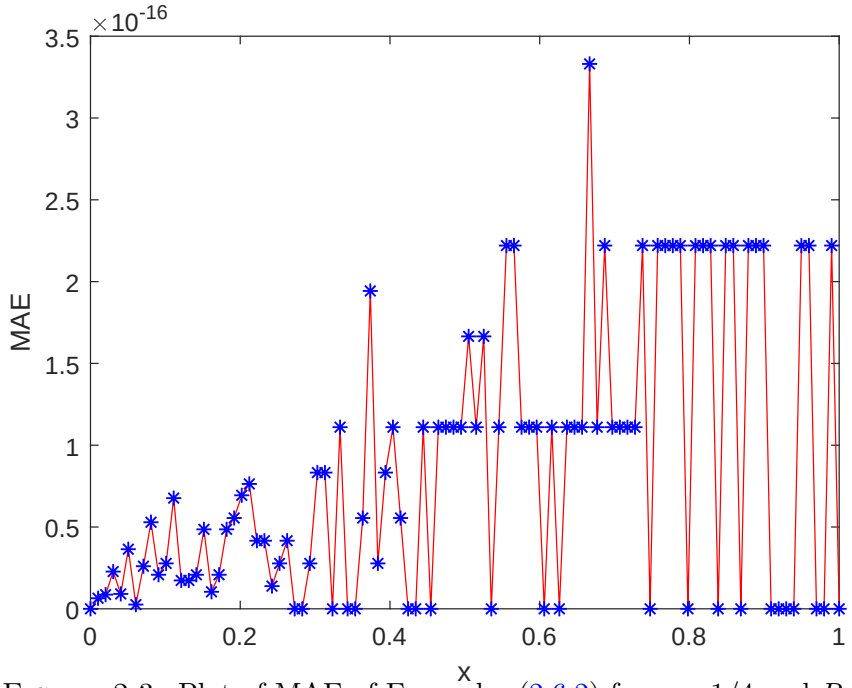

FIGURE 2.3: Plot of MAE of Examples (2.6.2) for $\gamma = 1/4$ and $R = 3$.

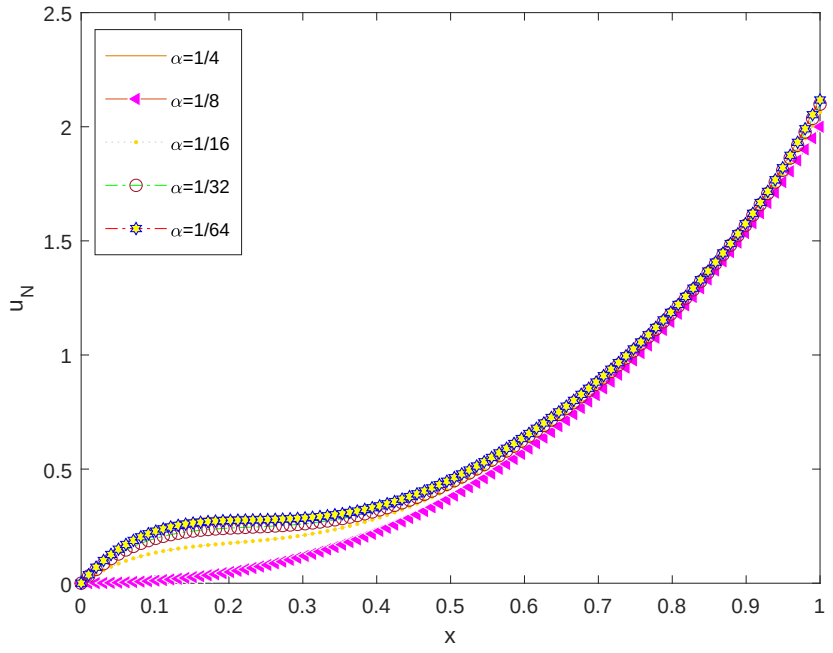

FIGURE 2.4: Plot of the approximate solution for different values of γ for Examples (2.6.2).

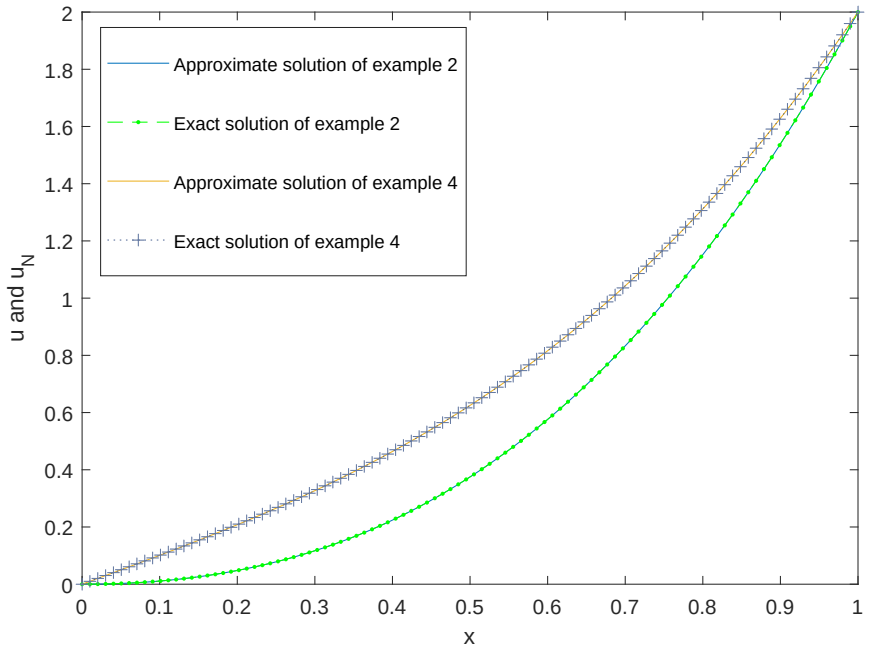

FIGURE 2.5: Plot of the exact versus approximate solution of Examples (2.6.2) and (2.6.4).

TABLE 2.2: Comparison of MAEs for Example 2.6.2 with the method proposed in [1] for different value of N.

N	Present Method	Method [1]
2	$5.551121e-17$	$2.2891e-02$
3	$2.77556e-17$	$2.0455e-16$

Example 2.6.3. Consider the nonlinear case of the problem with $\gamma = 1/2, n = 1$,

$$\begin{aligned}\int_0^x \frac{(x-t)^{-\gamma}}{\Gamma(\gamma)}\mathcal{D}^n(u(t))dt - q(x)u(x) + \int_0^x (x)^{1/2}\mathcal{G}(u(t))dt \\ = \frac{Sinh^{-1}(\sqrt{x})}{\sqrt{\Pi}\sqrt{(1+x)}} - \sqrt{x}(-x + (1+x)\ln(1+x)) \\ - \ln(1+x)(2\sqrt{x} + 2x^{3/2} - (\sqrt{x} + 2x^{3/2})\ln(1+x)),\end{aligned} \tag{2.68}$$

with $u(0) = 0$, and the exact solution is $\ln(1+x)$. In this case, the approximation solution is obtained by selecting different values of $N = 2, 3, 4, 5, 6, 7, 8, 9, 10$, and 11. MAEs corresponding to these cases are calculated, and the corresponding MAE comparison with other polynomials is shown in Table 2.3. We also plotted the graph of MAE versus N, as shown through Fig. (2.6). It can be observed that as N increases MAE tends to zero. Graph between the exact solution and approximate solutions is shown in Fig. (2.7).

TABLE 2.3: Comparison of MAEs for Example 2.6.3 with the method given in [1] for different value of N.

N	Present Method	Method [1]
3	2.383×10^{-3}	2.289×10^{-3}
4	4.320×10^{-4}	2.045×10^{-5}
5	3.728×10^{-5}	4.069×10^{-5}
6	1.834×10^{-6}	4.177×10^{-6}

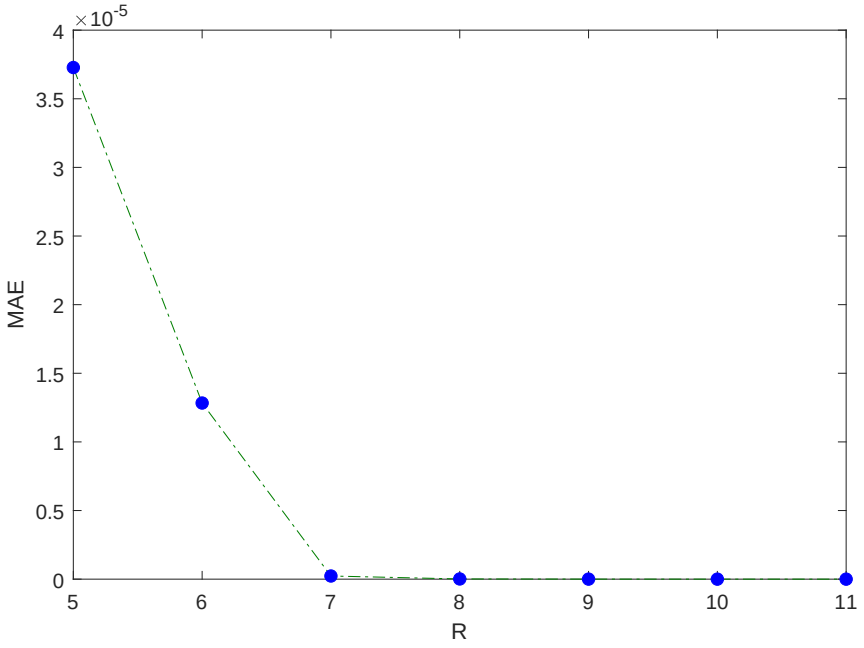

FIGURE 2.6: Plot of MAE of Example (2.6.3) for different values of N.

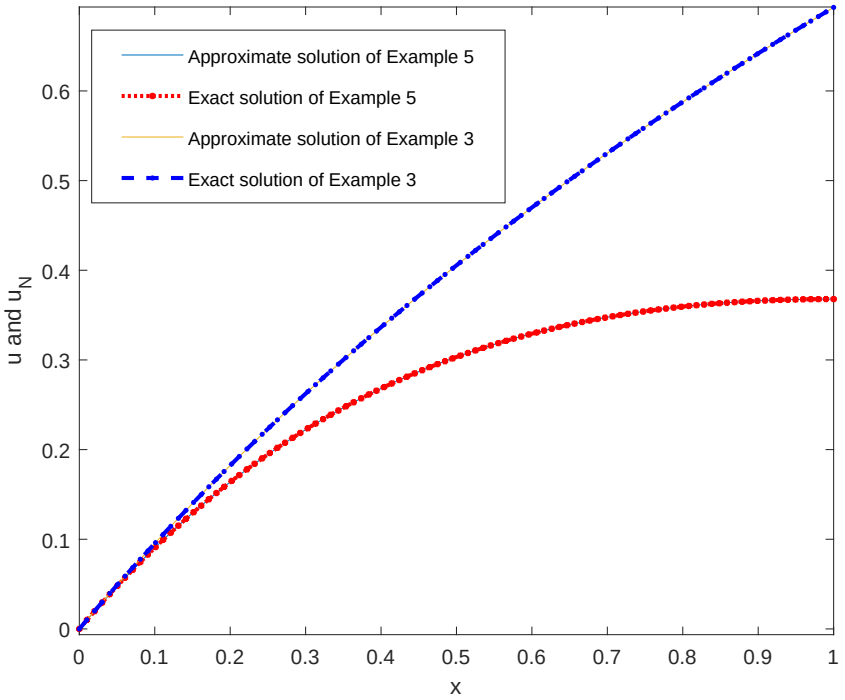

FIGURE 2.7: Plot of the exact versus approximate solution of Examples (2.6.5) and (2.6.3).

Example 2.6.4. Consider the problem with $\gamma = 2/3,\ n = 1,$

$$\int_0^x \frac{(d+(1-d)(x-t))^{-\gamma}}{\Gamma(\gamma)}\mathcal{D}^n(u(t))dt + \int_x^b \frac{(d+(1-d)(t-x))^{-\gamma}}{\Gamma(\gamma)}\mathcal{D}^n(u(t))dt$$
$$-u(x) - \int_0^x (x-t)^{-1/2}\mathcal{G}(u(t))dt - x - x^3 - \frac{4}{105}x^{3/2}(35+24x^2)$$
$$+\frac{3(x^{1/3}+\frac{27x^{7/3}}{14})}{\Gamma(1/3)} + \frac{3(1-x)^{1/3}+\frac{3}{14}(1-x)^{1/3}(2+3x+9x^2)}{\Gamma(1/3)}, \tag{2.69}$$

with $u(0) = 0$. The exact solution of the problem (2.6.4)is x^3+x. Here, as in previous cases, we calculate the MAE corresponding to different values of $N = 3, 4, 5$ and the case for $N = 4$ is shown in Fig. (2.8). We also depict the behavior of the solution by changing the value of $d = 1/4, 1/8, 1/16, 1/32$ and $1/64$. Furthermore, as d tends to zero, the approximate solution converges to exact solution which is shown in Fig. (2.9) . In Figure (2.5), a graph of the exact and the approximate solutions are given.

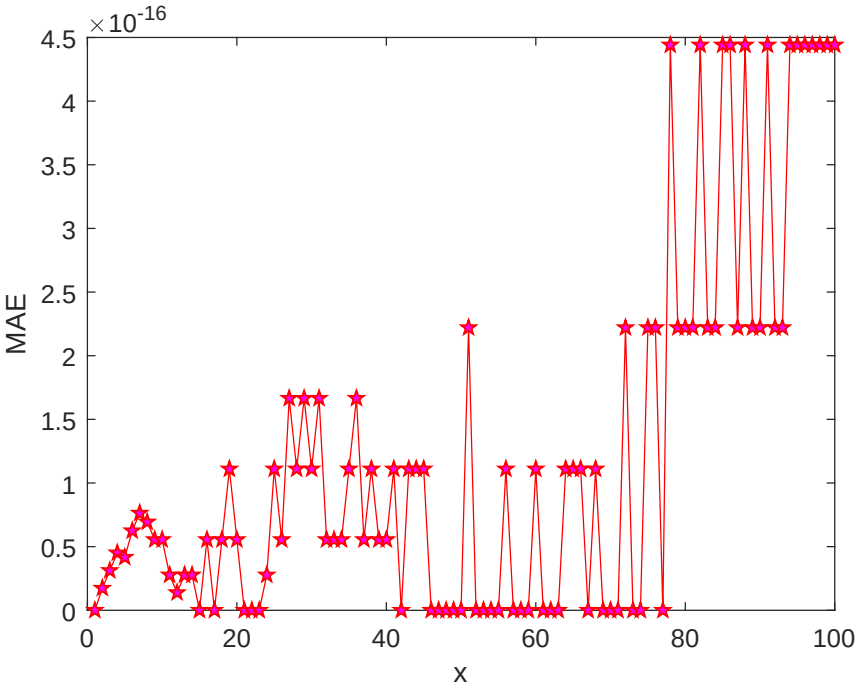

FIGURE 2.8: Plot of MAE of Example (2.6.4) for $\gamma = 2/3$, and N.

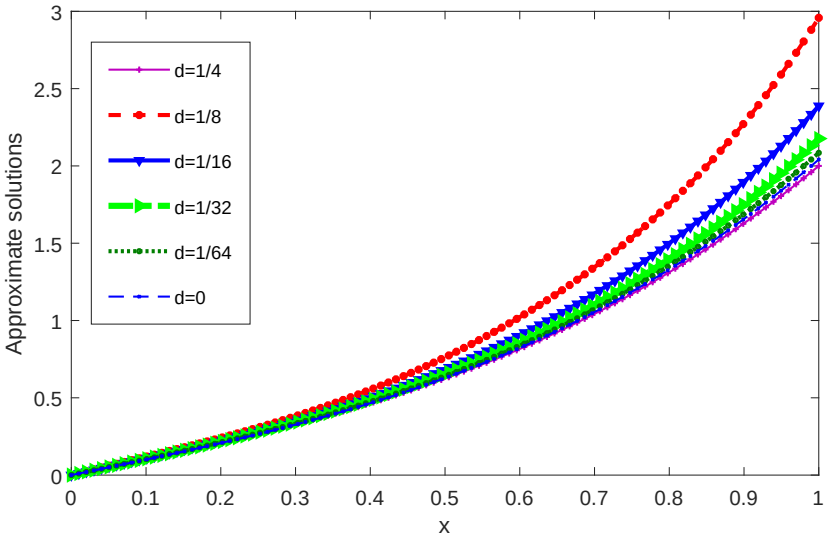

FIGURE 2.9: The numerical solution of Example (2.6.4) different values of d.

Example 2.6.5. Consider,

$$\begin{aligned}
&\int_0^x (1-\gamma)(x-t)\mathcal{D}^n(u(t))dt + \int_x^1 (1-\gamma)(t-x)\mathcal{D}^n(u(t))dt - u(x) \\
&- \int_0^x (x-t)^{-1/3}\mathcal{G}(u(t))dt \\
&= -e^{-x} - \frac{3(-3+x+e^{1-x}(1+x))}{4e} - \frac{3}{4}(1-e^{-x}(1+x)) - \\
&\frac{5(-1)^{1/3}e^{-x}\Gamma(2/3)\left(3e^x(-x)^{5/3} - (2+3x)(\Gamma(5/3) - \Gamma(5/3,-x))\right)}{9\Gamma(8/3)},
\end{aligned} \tag{2.70}$$

The problem (2.6.5) has the exact solution $u(x) = xe^{-x}$ with $u(0) = 0$. For the given problem, we find the approximate solution by varying the number of element in the basis and also calculate corresponding MAEs which are shown in Table 2.4. The graph of MAE verses N is shown in Figure (2.10). We notice that the MAE decreases as we increase N and for $N \geq 11$, no change in MAE is observed. In Figure (2.7), the graph of the exact and the approximate solutions are shown. We also plot the graph for the MAE for $N = 12$ and is shown in Fig. (2.11).

TABLE 2.4: Numerical solution for different values of M and N for Example (2.6.5).

N	Example (2.6.3)	Example (2.6.5)
3	2.383×10^{-3}	3.352×10^{-3}
4	4.320×10^{-4}	4.786×10^{-5}
5	3.728×10^{-5}	6.863×10^{-6}
6	1.833×10^{-6}	3.024×10^{-7}
7	2.295×10^{-7}	1.231×10^{-8}
8	1.284×10^{-8}	4.514×10^{-10}
9	1.417×10^{-9}	4.584×10^{-11}
10	6.199×10^{-10}	1.906×10^{-12}
11	2.467×10^{-10}	1.680×10^{-13}
12	3.215×10^{-10}	1.229×10^{-13}

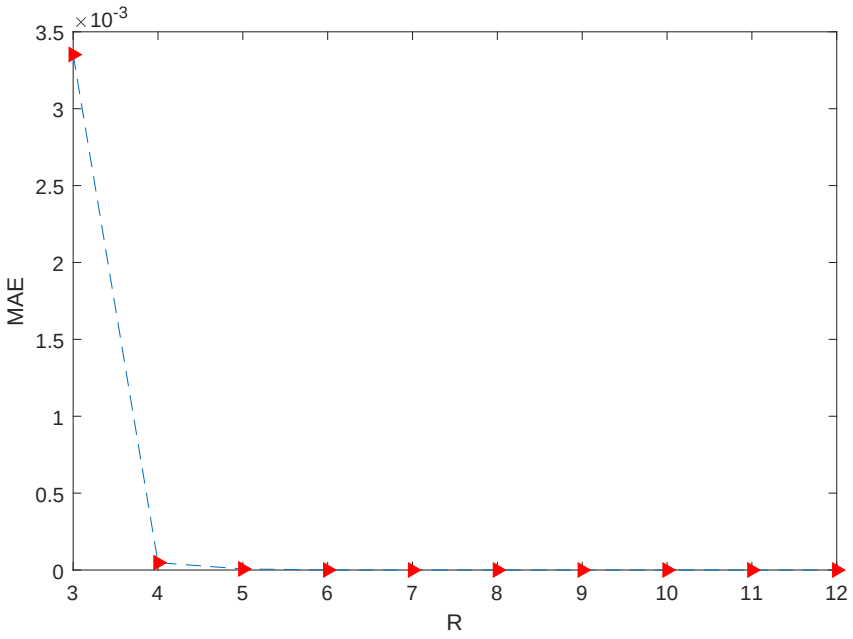

FIGURE 2.10: Plot of MAE for different values of N.

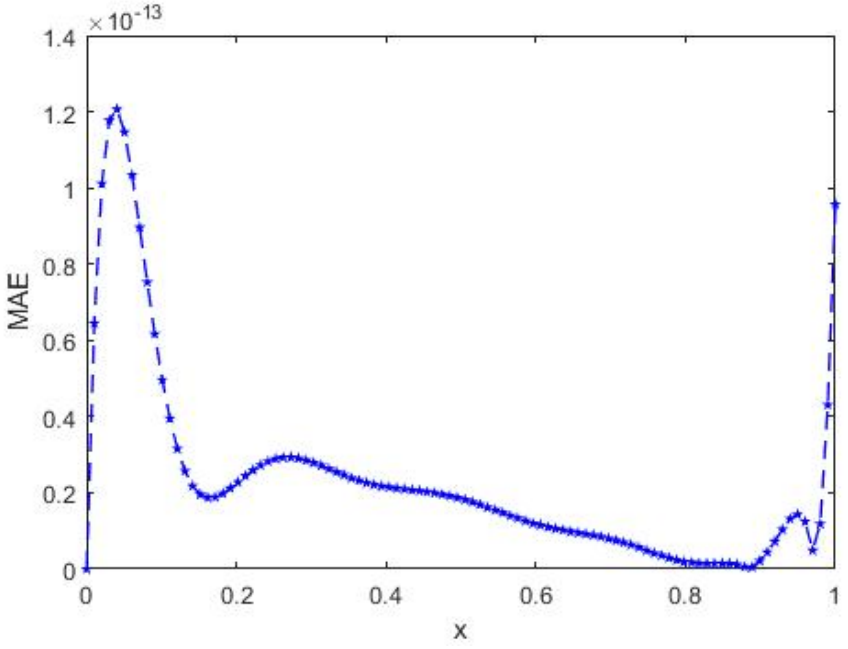

FIGURE 2.11: Plot of MAE Example (2.6.5) for $N = 12$.

2.7 Conclusions

A convergent collocation method is developed in this chapter for solving GFIDEs in terms of the B-operator. Jacobi poly-fractonomials are used as a basis in the proposed collocation method. The choice of the Jacobi poly-fractonomials helps to increase the accuracy in the approximated solution. The presented method works well on linear and nonlinear types of the GFIDEs and produces accurate solutions.

****